Proceedings of International Conference on Heat Exchanger Fouling and Cleaning VIII - 2009 (Peer-reviewed)
June 14-19, 2009, Schladming, Austria
Editors: H. Müller-Steinhagen, M.R. Malayeri and A.P. Watkinson

Published online
www.heatexchanger-fouling.com

FOULING IN HIGH SOLID CONTENT SUSPENSION– EFFECT OF NUCLEATING AIR AND BACKGROUND ELECTROLYTE

M. Riihimäki[1], U. Ojaniemi[2], T. J. H. Pättikangas[2], T. M. Pääkkönen[1], M. Manninen[2], E. Puhakka[2], E. Muurinen[1], C. J. Simonson[3], R. L. Keiski[1]

[1]University of Oulu, Department of Process and Environmental Engineering, Mass and Heat Transfer Process Laboratory, P.O. Box 4300, FI-90014 University of Oulu, Finland, markus.riihimaki@oulu.fi
[2]VTT Technical Research Centre of Finland, P.O. Box 1000, FI-02044 VTT, Finland
[3]University of Saskatchewan, Department of Mechanical Engineering, Saskatoon, SK, Canada

ABSTRACT

Particulate depositions formed on process surfaces of e.g. heat exchangers is a common problem in industry. Deposited material causes economical losses due to increased energy consumption, maintenance and cleaning. The particle deposition is often considered to include transport to the surface and adhesion on the surface dominated by surface forces such as DLVO interactions in aqueous systems. The fouling consists of complex phenomena that are not easy to distinguish experimentally. In this work, the effect of nucleation of dissolved air and the effect of background electrolyte on fouling are studied experimentally with slurries containing 6–50 wt-% of calcite ($CaCO_3$) particles, the primary size being about 0.8 µm. The experiments are performed in a laboratory set-up having a rectangular flow channel with heated walls. The bulk fluid temperature, heat flux, flow rate and solid content are varied in the experiments. Fouling is found to be induced by nucleating air at temperatures below boiling temperatures. The nucleation of air is eliminated by increasing the pressure in further experiments. The background electrolyte ($MgCl_2$) is found to have a strong effect on the dispersion properties and the fouling rate.

INTRODUCTION

Particle deposition mechanisms consisting of particle transport to the wall and particle adhesion on the wall have been widely studied (Epstein, 1997; Turner, 1993). It has been observed that the particle deposition rate has a maximum when particle charge is in a minimum or near zero (Hermansson, 1977) and a maximum may occur even when the particle and surface are oppositely charged (Williamsson *et al*., 1988). Adomeit and Renz (1996) introduced a method for particle transport and adhesion combined to a numerical model and further developed model accounting for hydrodynamically induced forces. For particle deposition, only a few studies have been done under boiling conditions (Turner and Klimas, 2000; Wen and Melendres, 1998; Bramson, 1995). Even fewer have been conducted in conditions where the nucleation of dissolved air has an effect on fouling (Yang *et al*., 2000). In some cases, the stability of the dispersed fluid is disturbed and undesirable fouling occurs.

In this study, a suspension containing ground particles of calcium carbonate is used in order to study particle deposition on a heated wall and how nucleating air and added background electrolyte have a marked effect on the mass deposition rate. The DLVO theory describes the force between charged surfaces interacting through a liquid medium. It combines the effects of the van der Waals attraction and the electrostatic repulsion due to the so called double layer of counterions. The theory is named after Derjaguin and Landau, Verwey and Overbeek. The XDLVO theory is an extension with the Lewis Acid-Base interactions that have marked effect on surfaces interacting in aqueous medium (van Oss, 1994). XDLVO theory was used in determining the forces affecting the particle, from which mass transfer coefficient for the particle was calculated according to methods of Spielman and Friedlander (1974) and Elimelech (1995). The CFD model (Ojaniemi *et al*. 2008) utilizing the mass transfer coefficients formed, is being validated using the experimental data of this study where background electrolyte was used and nucleation of air was eliminated.

EXPERIMENTAL SET-UP AND PROCEDURE

Experimental set-up

As crystals or particles deposit on the heat transfer surface, the overall heat transfer coefficient decreases. When the heat flux and wall temperature are constant, deposition of a resistive layer on the wall can be measured from the elevation of temperature by the thermocouple situated in the joint between heating block and a test material sheet forming a wall to the flow channel.

A schematic representation of the experimental set-up is given in Fig. 1. The construction material of the test set-up is AISI 316L. The set-up consists of a vessel of 150 dm^3

(1) that is open to the atmosphere and two flow loops: one for mixing the tank and another for a test section. A centrifugal pump (Kolmeks L-65B/2) (2) is connected to a frequency converter (Vacon NSX) in order to vary the pressure in the test section. The flow loop to the test section has flanges providing an option to connect in-line filters (3). Tap water is used for cooling the test fluid in a double pipe heat exchanger (4) (DN 25/50, 2.2 m) operated by a magnetic proportional valve (Bürkert 2832). It controls the temperature of the fluid entering the test section. A band heater (Mayer-vastus Oy, 2.5 kW) in the tank (1) is also connected to the same controller. The test section (5) is a rectangular flow channel having flow area of 15 x 100 mm and a length of 0.95 m following the entrance expansion and before exit contraction to the DN 20 pipes. The flow rate is measured by using a electromagnetic flow transmitter (Bürkert 8045) and controlled with a valve (Bürkert 2632). The tank (1) is equipped with measurement and control of pH value (Bürkert 8205) and conductivity (Bürkert 8225), which are connected to a magnetic on-off valve (Bürkert 0124) feeding the solution from a small dosing tank of 20 dm^3 (6) with the flow induced by hydrostatic pressure. In the test section, two removable sheet metal slabs of test material plates are mounted. Area of 0.1 m x 0.2 m is heated by a 25mm thick copper block where ohmic heaters having diameter of 6.5 mm (Watlow Firerod, 230V/1000W) are embedded. The heaters are connected to a power transformer (Teklab ACP100) to get constant, but adjustable heat flux. For three thermocouples (SKS Automaatio, K-type) channels have been drilled through the heating block. The thermocouples are measuring the wall temperature in the joint between the test material and the heating block. A uniform thermal contact in the joint is achieved with heat conductivity paste.

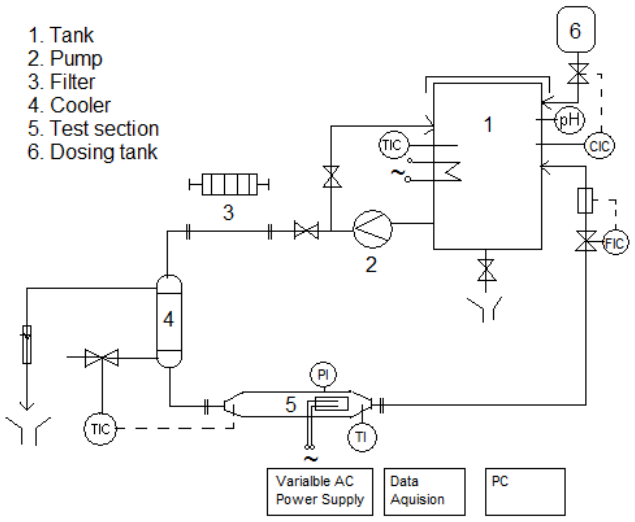

Fig.1. Schematic drawing of the test set-up.

Control and data acquisition system has been build using National Instruments Inc. cFP-2100 programmable automation controller with module components for measurement and control, and programmed with LabView 8.0 software. Measured values are saved using interval of 1 min without averaging or filtering the values. During an experiment, maximum fluctuation in the measured wall temperature is ±0.6% (±0.2°C) from the moving average, and in the bulk fluid temperature varies ±0.5% from the set point. The flow rate is ±8%, and the heat flux is within ±4% from the set point. Reproducibility of was confirmed with repeated tests.

Test fluid

In this investigation, dispersed suspension of ground lime stone having solid content (s.c.) of 50 wt-% was used. Ground lime stone (calcium carbonate) was used in experiments, because it is a common particle in hard waters causing fouling and its round shape can be considered spherical in particle models. The suspension was diluted in the experiments when lower s.c. 13 and 6 wt-% was used. Solid content was measured with Infrared Dryer (Mettler Toledo LP 16 connected to balance PM100). The conductivity of the suspension was 1.35 mS/cm and pH value was 8.4 at room temperature. The elemental composition analyzed by Inductively Coupled Plasma Optical Emission Spectroscopy (ICP-OES) and crystalline phases analyzed by X-ray powder diffraction spectroscopy (XRD, Siemens D5000) indicates that >98% of solid material is calcite with c.a. 1% of magnesium, and smaller amounts of other elements such as silicon, iron and aluminum. The particle size distribution (in Fig. 2) was measured with Mircromeritics SediGraph 5100. The volume based mean particle size was 0.82 ±0.07 µm, and 6% of the particles' mass were smaller than 0.2 µm which is below the detection limit of a sedigraph. The suspension was agitated when stored at room temperature. The storing period was restricted to less than four weeks in order to avoid settling and to keep the solid content homogeneous.

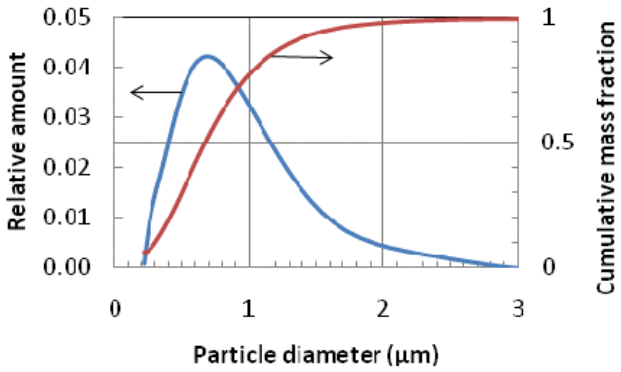

Fig. 2. Particle size distribution of the ground calcium carbonate suspension having the mean particle size of 0.82 µm and containing 6% finer particles than 0.2 µm.

The particle size and morphology were studied with electron microscopy. A droplet of the suspension was mixed in 1ml of ethanol in a decanter. The decanter was mixed in a sonic bath for 1 min. After mixing, a droplet of suspension was taken for an electron microscopy analysis. In Fig. 3. the Scanning Electron Microscopy (SEM, JSM-

6300F) image shows that the particles had a round or cubical shape with quite equal edge lengths of c.a. 0.8 µm. In the images, numerous small particles c.a. 0.2 µm and also few large particles c.a. 1 µm were identified.

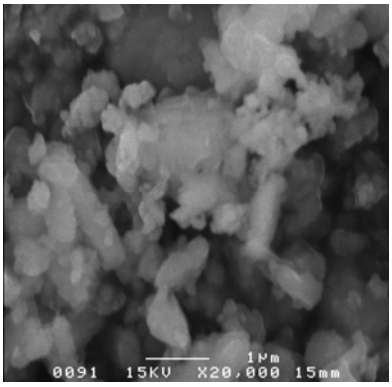

Fig. 3. Scanning electron microscopy image (SEM) of the ground calcium carbonate used in the experiments.

Zeta-potentials for the suspension were measured with Coulter Delsa 440SX. Measurements were done for the samples whose pH value was varied using NaOH or HCl. After the pH adjustment, the suspension was allowed to settle for 24h. The supernatant of the fluid was used in order to get correct particle concentration for a measured sample. If settling did not occur, the sample was centrifuged or filtered. The zeta-potential of the suspension was -25 mV and was independent of the pH between values 7 and 11.

Experimental procedure

The wall material in the experiments was stainless steel AISI 316L 2B (Outokumpu), mill surface which has a surface roughness of 0.28 ± 0.02 µm measured with R_a value (Mitutoyo SJ-201P) using measuring length 5 times 0.8 mm. The test material was cut into pieces (1.5 x 130 x 220 mm) suitable size for the test section. In order to clean the impurities from storage and machining, the test material was washed at c.a. 50°C in a solution containing 2 dm^3 water, 1 dm^3 ethanol (ETAX A, Altia Oy) and 60 ml detergent RBS 35 (R. Borghgraef S.A.) by first manually brushing the surfaces gently, then leaving the material to soak. After 2 hours of soaking, the material was brushed gently again, and then rinsed with warm tap water, followed by rinsing with de-ionized water.

After mounting the test pieces into the test section, the suspension of ground calcium carbonate was added to the tank and diluted to the desired solid content. The solid content of the diluted suspension was confirmed by the Infrared Dryer. The suspension was agitated by circulating it with the pump through the mixing loop and keeping the test loop closed. After the solution reached the temperature set in the test, the flow was directed to the test loop by opening the valve. An experiment started when the power was supplied to the heating blocks. The controlled variables in the experiments were heat flux, flow rate, and bulk fluid temperature. Solid contents of 50, 13, 6 wt-% were used in the experiments.

RESULTS AND DISCUSSION

Effect of nucleating air

In the experiments with dispersed s.c. 50 wt-% suspension, operating conditions were varied a follows: heat flux 0-55 kW/m^2, velocity 0.15-0.70 m/s and fluid temperature 30-80°C. As shown in Fig. 4, the deposition of particles was observed by elevation of temperature only when the temperature of the heated wall was more than 80°C. The mass deposition rate increased markedly when the temperature at the wall was more than 100°C. Any delay of the temperature elevation (referred also as induction period) in the initial phase of the experiments was not observed.

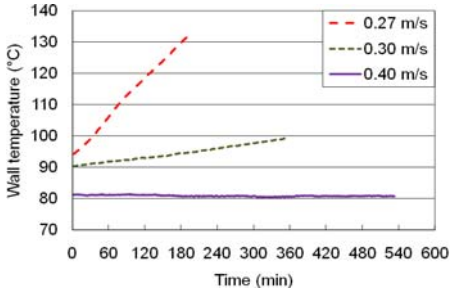

Fig. 4. Temperature evolution of the wall, when the deposition of particles occurs on the heated wall. The bulk fluid temperature was 60°C, heat flux 30 kW/m^2 and solid content 50 wt-%.

In order to exclude boiling from this study, the experiments were started in the conditions that gave the wall temperature between 80 and 95°C in the beginning of the experiment. The material deposited in the experiments was collected and analyzed with microscopy (Fig 5). With the microscopy the bubbles were observed in the deposited layer under the temperatures of boiling of water, it was concluded that the nucleation of dissolved air bubbles took place.

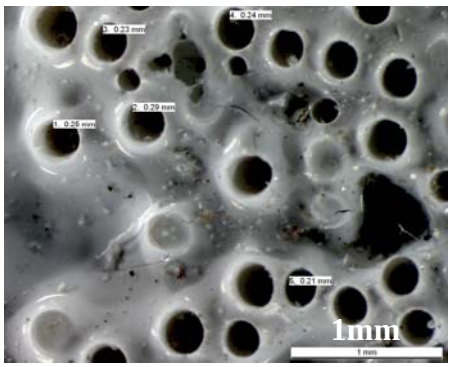

Fig. 5. The deposition formed in the fouling experiment with the suspension having s.c. 50 wt-%, fluid temperature 60°C, heat flux 34 kW/m^2, and flow velocity 0.3 m/s.

It was observed that the deposition was thicker around a bubble. When the deposition continued, the bubble had possibility to get trapped and a hole or duct with no

deposition started to form in the place of the bubble. If the bubble was small enough, the deposition grew over the bubble and covered it. Bubbles nucleated on the already deposited material. The diameters of the bubbles were measured optically and the average was calculated from 5 randomly selected locations. The diameter of holes increased strongly with increasing wall temperature (Fig. 6). It was also found that the mass deposition rate increased with increasing wall temperature but not linearly as the diameter of holes. It is proposed that when the bubbles grow bigger they start to move on the surface or even detach from the surface retarding the deposition of particles.

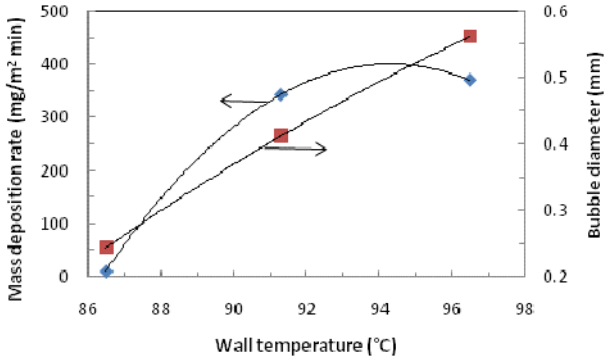

Fig. 6. Mass deposition rate (◆ left axis) and bubble diameter (▪ right axis) as a function of the wall temperature. The fluid temperature was 60, 65 and 70°C corresponding to the wall temperatures 87, 92 and 97°C, and flow velocity 0.3 m/s, and heat flux 30 kW/m^2.

In the experiments with the varied heat flux (in Fig. 7.), the bubble size increased from 0.32 to 0.42 mm when the heat flux increased from 30 to 37 kW/m^2, when the fluid velocity was 0.3 m/s. The mass deposition rate increased with increasing heat flux with fluid velocities 0.30 and 0.27 m/s.

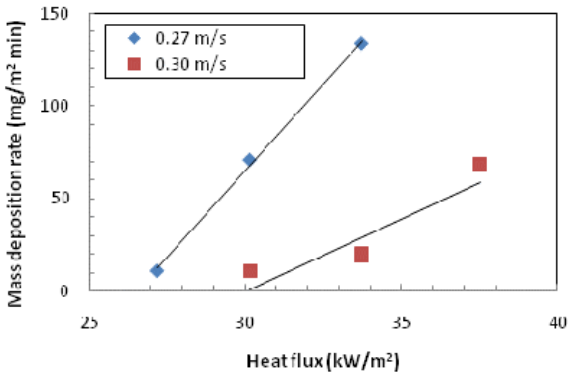

Fig. 7. The mass deposition rate as a function of the heat flux with the fluid velocities 0.27 m/s (◆) and 0.3 m/s (▪) with constant fluid temperature 60°C.

The nucleation of air bubbles on the wall is due to the solubility difference of air in the bulk fluid and on the heated wall. Fig. 8 shows the solubility of air in water as a function of temperature. A heated wall has a smaller solubility compared to the bulk fluid and after a while bubbles nucleate on the surface. It can also be noticed that the solubility of air is a non-linear function of temperature. This implies that in the experiments with constant temperature gradient (in Fig. 6), the difference in water solubility gradient increases with increasing fluid temperature above 60°C. Thus, the observed increase of the bubble size is caused by the increasing solubility gradient. In Fig. 7 with varied heat flux, the solubility gradient of air is increased with increasing temperature gradient. Also the increase in bubble size was observed with increasing heat flux.

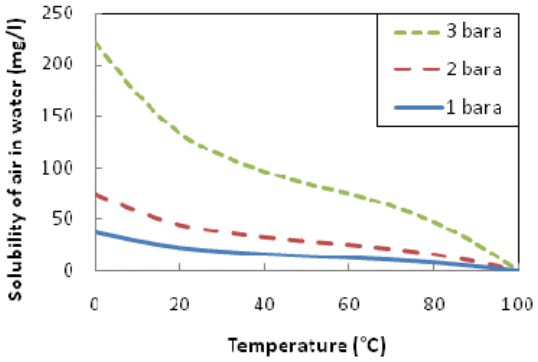

Fig 8. Solubility of air in water as a function of temperature.

Henry's law gives a linear relationship between pressure and the solubility of a gas in liquid at a specified temperature:

$$p_A = H_c x_A, \quad (1)$$

where p_A is the partial pressure of the gas A, H_c is Henry's constant of the gas and x_A is the mole fraction of the solute in the liquid phase. Bubble formation from a supersaturated solution takes place when the bubble size overrides critical nucleus size

$$r_c = 2\sigma/\Delta p, \quad (2)$$

where σ is the surface tension of the fluid and Δp pressure difference across the interface (Young-Laplace equation).

Different alternatives exist for the elimination of the bubble formation: Addition of chemical to increase surface tension would increase the critical nucleus size and make nucleation less probable. Dissolved gases could be removed from the test fluid e.g. by boiling the fluid before an experiment in the tank by heating it up to the boiling temperature or by using vacuum to lower the boiling point. Handling the steam or boiling the fluid were found to be time consuming and were also found to have safety factors to be considered. An option is to elevate the pressure in the test section so that nucleation does not take place on the heated wall. The elevated pressure was chosen to prevent the nucleation of dissolved air.

Solubility of air in water may not be accurate with the suspension that has dissolved salts, dispersion chemicals etc. In addition, the nucleation kinetics is not known. In this

study, the pressure dependency of the fouling rate was studied in order to find out how nucleation of the bubbles from further experiments can be eliminated and how much the pressure should be increased in order to compensate for the solubility decrease due to the temperature increase in the test section. The pressure was measured at the test section and was adjusted with the frequency converter connected to the pump.

In Fig. 9 the mass deposition rate decreased with increasing pressure. The mass deposition rate decreased with increasing pressure because the solubility of the air increased due to the pressure increase. With higher pressures solubility of air is not exceeded anymore and bubbles are not observed in the optical inspection of the fouling layer at the end of the test.

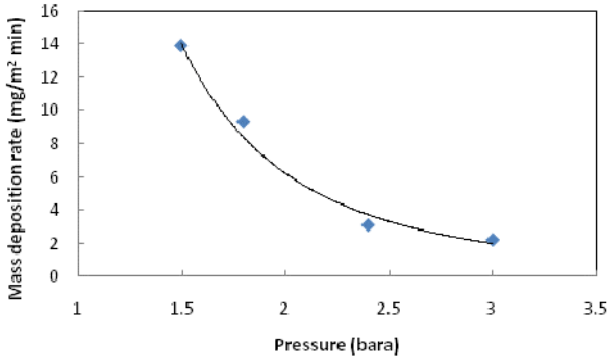

Fig. 9. Mass deposition rate as a function of pressure with velocity 0.3 m/s, fluid temperature 65°C and heat flux 34 kW/m^2. Temperature at the heated wall was 93°C in the beginning of each test.

Effect of electrolytes

In the industrial processes, fouling may start in many cases without any noticeable reasons. Even a small amount of a trace element may initiate fouling. The colloidal stability of the particles may be disturbed by an electrolyte. In this study, an electrolyte (Na^+, Mg^{2+}) was added to the suspension and the mass deposition rate was studied studied in the conditions where air did not have possibility to nucleate on the heated wall and did not have effect on mass deposition rate. Adding $NaHCO_3$ and $MgCl_2$ salts were selected to increase background electrolyte concentration of the test solution. $MgCl_2$ was selected to increase also hardness of the solution that is main impurity electrolyte $CaCO_3$ containing waters.

The zeta-potential of the test fluid was initially -25 mV, independent of the pH value. The zeta-potential of the test fluid with added electrolytes: $MgCl_2 \cdot 6H_2O$ (J.T. Baker, Prolabo 25 107.292) and $NaHCO_3$ (Merck, Ph Eur) were also measured. In Fig. 10 the zeta-potentials for these solutions are given as a function of the electrolyte concentration. A small amount of $MgCl_2$ such as 0.5 g/l decreased the zeta-potential markedly and a concentration of 5 g/l in the test fluid decreased the zeta-potential close to zero. Adding a small amount of $NaHCO_3$ causes the zeta-potential to decrease significantly to the value of -38 mV, but further addition to a concentration of 5 and 15 g/l zeta-potential started to increase but not lower than initial value -25 mV.

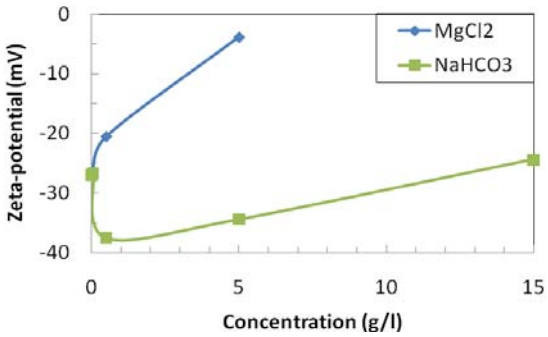

Fig. 10. Zeta-potential of the suspension when $MgCl_2$ (◆), and $NaHCO_3$ (▪) are added.

The settling of the suspension was observed (in Fig. 11) to depend on both the added electrolyte and its concentration. The suspension settles when the concentration of $MgCl_2$ is grater than 0.5 g/l $MgCl_2$ while the concentration of $NaHCO_3$ needs to 15g/l before the suspension settles.

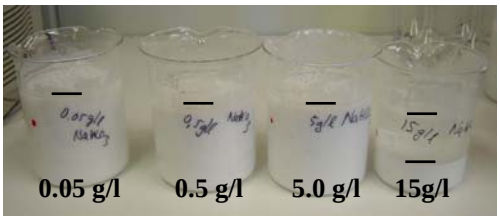

a) settling of the suspension with $NaHCO_3$ concentration more than 5 g/l

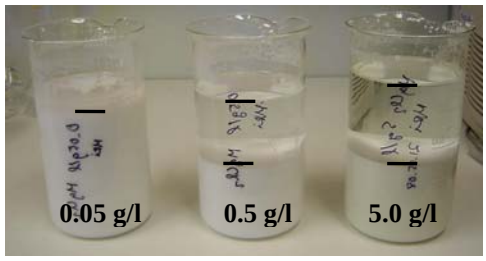

b) settling of the suspension with $MgCl_2$ more than 0.05 g/l

Fig. 11. Addition of an electrolyte to the dispersed suspension.

Adding of the electrolyte to the suspension increased the viscosity of the suspension markedly. Due to this increase in viscosity, experiments could not be conducted with s.c. 50 wt-%. The suspension was diluted with de-ionized water to the s.c. 13.0 wt-%. $MgCl_2$ was added to get concentration of 0.53 g/l in the diluted suspension, to maintain the conductivity level, the level as the suspension had before the dilution. In Fig. 12 is seen a non-fouling period before the addition of $MgCl_2$, then an increase of the wall temperature caused by the viscosity increase due to the salt addition, and finally the steady fouling period.

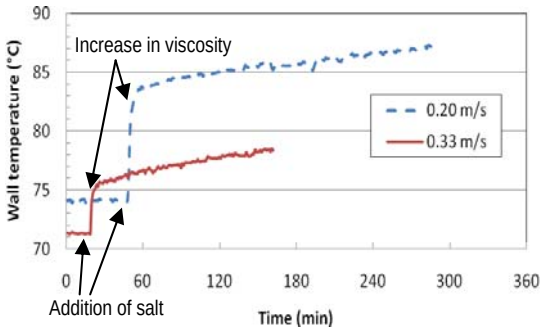

Fig. 12. Experiments with the suspension diluted to s.c. 13.0 wt-%, with $MgCl_2$ addition at the times 20 min and 60 min from the start. A non-fouling period, temperature elevation due to salt addition and steady period of deposition of particles was observed.

Because the increase in the viscosity and the deposition of particles were observed at the same time, they may have common affecting factors. The zeta-potential of particles decreased from -25 mV to -18 mV when 0.5 g/l $MgCl_2$ is created (Fig. 10) and the settling of the suspension is also observed (Fig. 11). This indicates that the interaction forces between particles became stronger and the deposition of the particles also became possible.

The mass of the deposited particles was measured after each experiment. The deposited material was scraped off from the test surface, dried at 105°C over night and weighed. The elevation of the wall temperature and accumulated mass is given in Fig. 13. Reasonable correlation was found between temperature elevation of the wall and accumulated mass weighed after the experiments.

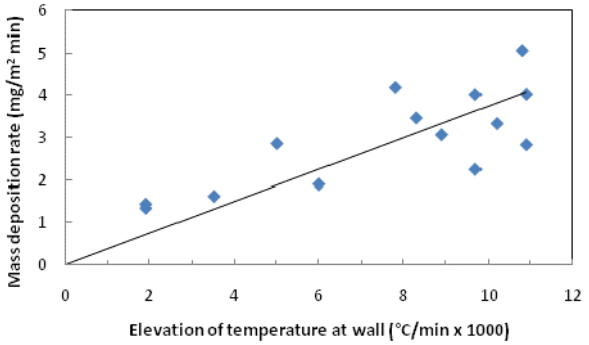

Fig. 13. Mass deposition rate as a function of the elevation in the surface temperature.

The average composition of the deposited material corresponds to 66 wt-% of $CaCO_3$ and 34 wt-% of H_2O, according to the estimated thermal conductivity of the deposited material. The composition was estimated using conductivity of the water (0.6 W/mK) and calcite (2.0 W/mK) assuming that the water is filling the volume between the packed particles, the void fraction of the deposited material is 0.34.

In Fig. 14, the mass deposition rate is found to decrease with increasing fluid velocity. Increase in velocity enhances the shear forces and also the turbulence at the wall which promotes particle re-entrainment and deposition rate is decreased.

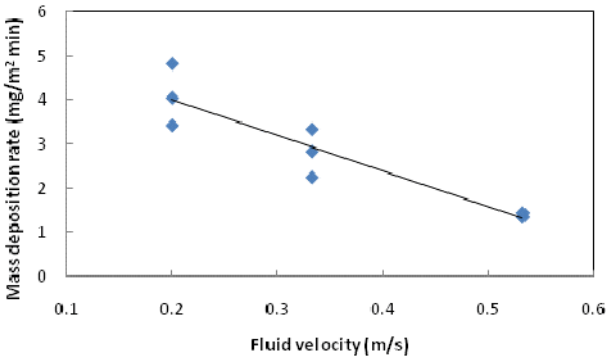

Fig. 14. Mass deposition rate as a function of fluid velocity with s.c. 13 wt-%, 0.53 g/l $MgCl_2$ added, fluid temperature 60°C and heat flux 21 kW/m^2.

In Fig. 15, the mass deposition rate increases with increasing heat flux as well as the increasing temperature gradient between the heated wall and the bulk fluid. Thermophoresis or the Sorét effect is a transport phenomena, where small or colloidal particles drift along a temperature gradient. Typically, particles deplete from regions of high temperature. Thermophoresis is proposed to have an effect on the particulate deposition in aqueous systems but there is no clear understanding even of its order of magnitude in the deposition models (Ojaniemi *et al.*, 2008). The mass deposition rate has no clear correlation with the fluid temperature or the initial wall temperature. The temperature has usually a strong effect on chemical reactions and crystallization rate and on solubility of gases, but in particle transport and adhesion, the effect of fluid temperature may be weak and thus was not clearly obtained in these experiments.

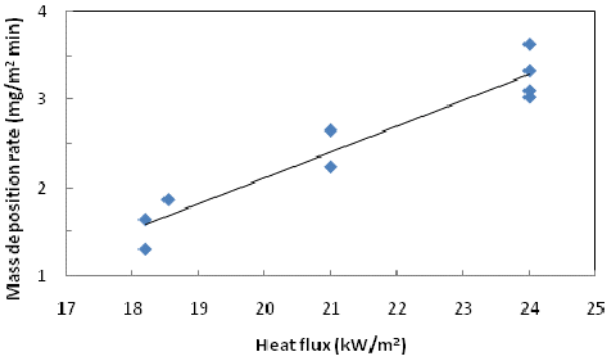

Fig. 15. Mass deposition rate as a function of heat flux with s.c. 13 wt-%, 0.53 g/l $MgCl_2$ added, fluid temperature 60°C and flow rate 0.3 m/s.

The mass deposition rate was found to increase with the decreasing solid content when the suspension was diluted with de-ionized water from 50 wt-% to 16, 13, and 5.9 wt-% and the conductivity of the fluid was increased to the value before the dilution of the suspension by adding

$MgCl_2$. The dilution of the suspension had a strong effect on the dispersion properties of the fluid. In order to vary solid content by dilution, constant conductivity may not be reasonable.

Adhesion of particles by XDLVO interactions

A model for particulate fouling is regarded as the serial process of the particle transport to the vicinity of the wall, and adhesion on the wall controlled by XDLVO forces. A detailed description of the CFD model can be found in Ojaniemi *et al.* (2008), where the deposition rate controlled by adhesion for the Brownian particles in the presence of repulsive colloidal forces has been implemented as a boundary condition using a mass transfer coefficient, which combines the XDLVO-theory and the methods of Spielman and Friedlander (1974) and Elimelech *et al.* (1995). I this paper, the model for the mass transfer coefficient was further developed to include the water permittivity dependence on temperature (Handbook of Chemistry and Physics, 1998) and on the particle distance from the wall surfaces (Podgornik *et al.*, 1987; Teschke *et al.*, 2001 The dielectric permittivity of water describes the ability of water to polarize in response to the electric field, and thereby reduce the total electric field in the near-wall region.

In Figure 16, the mass transfer rate is shown for two particle sizes as a function of surface temperature calculated with three ion strengths of the fluid. The values for parameters used in XDLVO-model when calculating the mass transfer coefficient are based on the experiments. The increase of ion strength increases markedly the mass transfer rate that enforces the fouling. The result corresponds with the experimental results, where addition of electrolyte has strong effect on mass deposition rate.

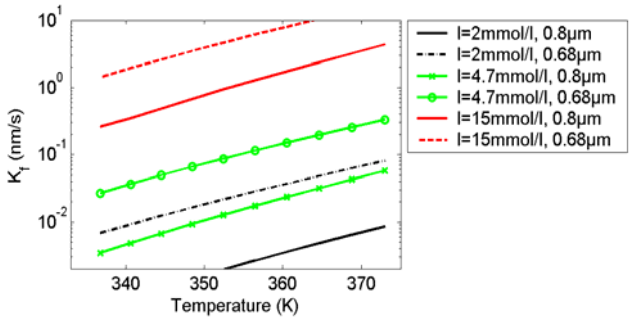

Fig. 16 Mass transfer coefficient as a function of the wall surface temperature. The rate calculated with variations of ion strength (I) is shown for two particle sizes (0.8 µm, 0.68 µm).

The XDLVO theory is based on the interaction energies of van der Waals, the electrical double layer and the acid-base interaction, which all depend on the particle size. The mass transfer coefficient increases with decreasing particle size, as shown in Fig. 16. Thus, the smaller the particle, the more likely it will adhere to the surface. In Fig. 17 the dependency of mass transfer coefficient on the particle size at a temperature at 72°C is presented along with the particle size distribution of the test fluid. Only a minor fraction of the particles have significant mass transfer coefficient in order to have effect on the growth of the deposition layer and thus be responsible of the fouling.

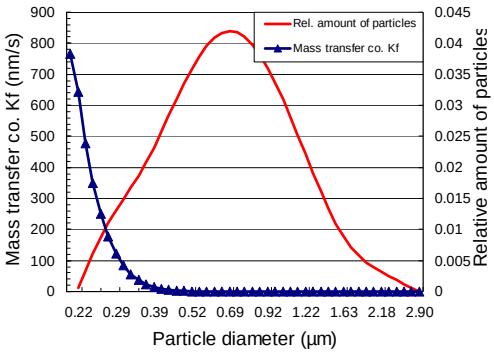

Fig. 17 Mass transfer coefficient as a function of particle size calculated at temperature 345K and the particle size distribution of the test fluid.

A validation of a CFD model developed for particulate fouling has been started with the results of the experiments carried out with background electrolyte in the conditions where the nucleation of air bubbles was eliminated.

CONCLUSIONS

Particulate deposition on the heated surface was studied in a presence of dissolved air and an added electrolyte, which may be reasons why in certain conditions fouling initiates. To avoid the initiation of fouling, would benefit industry in smooth operation of processes with reduced maintenance and energy costs. The nucleation of dissolved air from flowing fluid on a heated steel AISI 316L 2B surface induced particle deposition from a high solid content suspension that contained 50 wt-% ground calcium carbonate particles of submicron size. Keeping the surface temperature below the boiling point is not enough in avoiding the initiation of fouling, if saturation of dissolved air is reached and nucleation of air bubbles occurs. Elevation of the pressure is suggested to diminish already nucleated bubbles and to increase the dissolution of gases. In addition to the effect of bubbles, it was observed that added background electrolyte disturbed the stability of the suspension: $MgCl_2$ had a strong ability to induce fouling compared with $NaHCO_3$. The interaction forces between particles became stronger and also the deposition of the particles became possible. Induction time for the particulate fouling was not observed. Implementation of surface forces into CFD fouling model can be done by using mass transfer coefficient based on XDLVO theory.

NOMENCLATURE

p_A partial pressure of the gas A, Pa
H_c Henry's constant of the gas, 1/mol
x_A the mole fraction of the solute in the liquid phase
rc critical nucleus radius, m
σ surface tension of the fluid, N/m
Δp pressure difference across the interface, Pa

SEM scaning electron microscopy
TEM transmission electron microscopy
XRD X-ray diffraction

ACKNOWLEDGEMENTS

This study was financially supported by Tekes and industrial partners in the MATERA ERA-Net cooperation.

REFERENCES

Adomeit P., and Renz U., 1996. Deposition of fine particles from a turbulent liquid flow: Experiments and numerical predictions. *Chemical Engineering Science*, Vol. 51, No. 13, pp. 3491-3503.

Adomeit P., and Renz U., 2000. Correlations for the Particle Deposition Rate Accounting for Lift Forces and Hydrodynamic Mobility Reduction. *The Canadian Journal of Chemical Engineering*, Vol. 78, pp. 32-39.

Bramson D., Hasson D., and Semiat R., 1995. The roles of gas bubbling, wall crystallization and particulate deposition in CaSO4 scale formation. *Desalination* Vol. 100, pp. 105-113.

Epstein N., 1997. Elements of particle deposition onto nonporous solid surfaces parallel to suspension flows *Experimental Thermal and Fluid Science* Vol. 14, No. 4, pp. 323-334.

Elimelech M., Greory J., Jia X., Williams R.A., 1995. *Particle Deposition and Aggregation - Measurement, Modelling and Simulation*, Elsevier.

Handbook of Chemistry and Physics, 1998, CRC Press, Boca, Raton.

Hermansson H-P., 1977. Electrokinetic Deposition of Waterborne, Particulate FeO(OH) and MnO_2 on Stainless Steel Surfaces. *Chemica Scripta*, Vol. 12, 102-108.

Ojaniemi, U., Pättikangas T., Riihimäki M., Manninen M., 2008. CFD Model for Particulate Fouling - Modeling Particle Adhesion on Surface with XDLVO Theory, 6th International Conference on CFD in Oil & Gas, Metallurgical and Process Industries, SINTEF/NTNU, Trondheim, Norway.

Podgornik R., Cevc G., Zeks B., 1987. Solvent structure effects in the macroscopic theory of van der Waals forces, *Journal of Chemistry Physics* 87, 5957

Teschke O., Ceotto G., Souza E.F., 2001. Interfacial water dielectric-permittivity-profile measurements using atomic force microscopy, *Physical Review E.*, Vol. 64 , 011605-1 - 10

Turner C.W., 1993. Rates of Particle Deposition From Aqueous Suspensions in Turbulent Flow; a Comparison of Theory with Experiment, *Chemical Engineering Science*, Vol. 48, No. 12, pp. 2189-2195.

Turner C.W., Klimas S.J, 2000. Deposition of magnetite particles from flowing suspensions under flow-boiling and single-phase forced-convective heat transfer. *The Canadian Journal of Chemical Engineering,* Vol. 78, No 6, pp. 1065-1075.

van Oss C.J., 1994. *Interfacial Forces in Aqueous Media.* Marcel Dekker, Inc.

Wen L., and Melendres C.A., 1998. On the mechanism of hematite deposition on a meta surface under nucleate boiling conditions. *Colloids and Surfaces A: Physicochemical and Engineering Aspects*, Vol. 132, pp. 315-319.

Williamson R., Newson I., and Bott T. R., 1988. The deposition of Haematite particles from flowing water. The *Canadian Journal of Chemical Engineering*. Vol. 66, pp. 51-54.

Yang Q., Ding J., and Shen Z., 2000. Investigation on fouling behaviours of low-energy surface and fouling fractal characteristics. *Chemical Engineering Science* Vol. 55, pp. 797-805.